Engineering a Molecular Model for Water Phase Equilibrium over a Wide Temperature Range

Georgios C. Boulougouris,[†,‡] Ioannis G. Economou,[*,†] and Doros N. Theodorou[†,§]

Molecular Modelling of Materials Laboratory, Institute of Physical Chemistry, National Research Centre for Physical Sciences "Demokritos", GR 15310 Aghia Paraskevi Attikis, Greece, Department of Chemical Engineering, University of Patras, GR 26500 Patras, Greece, and Department of Chemical Engineering, National Technical University of Athens, GR 15773 Zografos, Athens, Greece

Received: August 7, 1997; In Final Form: October 31, 1997

The pure water phase equilibrium is calculated over a wide temperature range using the Gibbs ensemble Monte Carlo method with simple two-body molecular models. The Ewald summation method is used to account for the long-range Coulombic interactions. Coexisting liquid and vapor densities and vapor pressure at different temperatures are calculated explicitly. A new expression is developed for the direct calculation of pressure suitable for systems where the Ewald method is used. To improve agreement with experimental data, a simple scaling procedure is proposed that allows reparametrization of the molecular models without the need for additional calculations. Critical constants, second virial coefficient, and heat of vaporization are calculated from the different models. Finally, water structure is examined at low and high temperature. In all cases, comparison with experimental data is shown.

Introduction

Despite the extensive use of water for many technological applications and its importance for several biological processes, it is not fully understood yet how molecular structure and microscopic mechanisms affect macroscopic thermodynamic and other properties. This information is crucial for a variety of traditional and novel chemical engineering applications where water is used at extreme conditions including its critical and supercritical region, for example for oxidation purposes and as a reaction medium.[1]

Molecular simulation advances over the past decade made possible the calculation of macroscopic properties of pure compounds and mixtures where interactions are far from ideal, using appropriate molecular models.[2] To this extent, thermodynamic properties and phase equilibria of aqueous systems have been studied extensively using simple models.[3−7] Almost all of the semiempirical molecular models currently available for water were developed in order to calculate accurately thermodynamic (liquid density, heat of vaporization, etc.) and structure (pair distribution functions) properties at ambient conditions (20−40 °C) which are of most interest for biological and chemical applications. As a result, predictions from these models at higher temperature are not in good agreement with experimental data.

In this work, two simple molecular models, the simple point charge (SPC)[8] and the extended SPC (SPC/E)[9] models, are used to calculate pure water vapor−liquid equilibrium over a wide temperature range (300−610 K). Long-range interactions are taken into account through the Ewald summation technique.[10] The Gibbs ensemble Monte Carlo method[11] is utilized that allows direct simulation of the coexisting phases. In this way, the vapor and liquid densities as well as the vapor pressure at different temperatures are obtained. An analytical expression is developed to calculate the equilibrium pressure. Simulation results are compared with literature values using the same models.

A simple methodology is proposed for the reevaluation of the molecular model parameters using a scaling procedure so that better agreement with experimental saturated densities and vapor pressure is obtained. The new parameters can be used for reliable mixture calculations. This methodology is quite general and can be used for other components and for different target properties. A similar method was used, for example, for carbon dioxide.[12] Finally, second virial coefficient, enthalpy of vaporization, and radial distribution functions are calculated using the different molecular models.

Model Development

The focus of this work is to use simple molecular models to calculate pure water vapor−liquid equilibrium properties. Several semiempirical two-body potentials have been proposed in the literature that are variations of the Bernal and Fowler model.[13] According to these approaches, water is modeled as a Lennard-Jones sphere located on the oxygen atom with two positive partial charges located on the two hydrogens and a negative partial charge located either on the oxygen atom (three-site model) or on the dichotomy of the H−O−H angle (four-site model, Figure 1). To evaluate the interactions between two water molecules, 9 distances are required for the three-site models and 10 distances for the four-site models, resulting in an increase in the computational time. Model parameters are usually evaluated from ab initio calculations and are adjusted in order to accurately represent thermodynamic properties of liquid water at 25 °C.[3]

More complicated molecular models have been proposed where many-body effects are taken into account by introducing point polarizability in the model.[14−16] Despite the increased

* Author to whom all correspondence should be addressed. E-mail: economou@cyclades.nrcps.ariadne-t.gr. Fax: +30-1-6511766.
† National Research Centre for Physical Sciences "Demokritos".
‡ National Technical University of Athens.
§ University of Patras.

S1089-5647(97)02582-0 CCC: $15.00
Published on Web 01/22/1998

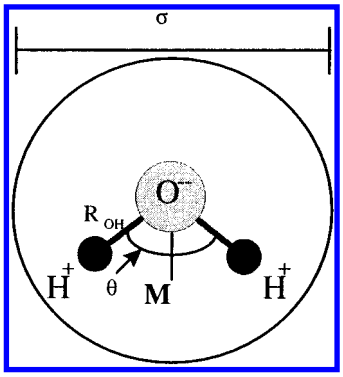

Figure 1. Schematic representation of the molecular model for water used in this work.

complexity of these models and the considerably higher computational time required, the improvement concerning phase equilibrium predictions is minimal.[7,17]

In this work, two three-site models are used for phase equilibrium calculations: the SPC[8] and the SPC/E.[9] The Ewald summation method is used to account for the long-range intermolecular interactions. For both models, the intermolecular energy can be expressed in reduced form as

$$\tilde{E}_{tot} = \frac{E_{tot}}{\epsilon} = \frac{q^2}{\epsilon\sigma}\frac{\sigma}{L}\sum_{i<j}^{N}\sum_{\alpha}^{m}\sum_{\beta}^{m} S_i^{\alpha} S_j^{\beta}\,\mathrm{erfc}\left(\frac{\lambda r_{ij}^{\alpha\beta}}{L}\right)\left(\frac{L}{r_{ij}^{\alpha\beta}}\right) +$$

$$\frac{1}{2}\frac{q^2}{\epsilon\sigma}\frac{\sigma}{L}\sum_{i}^{N}\sum_{\alpha}^{m}\sum_{\beta\neq\alpha}^{m} S_i^{\alpha} S_i^{\beta}\left(\mathrm{erfc}\left(\frac{\lambda r_{ii}^{\alpha\beta}}{L}\right)\left(\frac{L}{r_{ii}^{\alpha\beta}}\right) - \left(\frac{L}{r_{ii}^{\alpha\beta}}\right)\right) +$$

$$2\pi\frac{q^2}{\epsilon\sigma}\frac{\sigma}{L}\sum_{\vec{k}\neq 0}\frac{1}{k^2L^2}\exp\left(-\frac{k^2L^2}{4\lambda^2}\right)[(\sum_{i}^{N}\sum_{\alpha}^{m} S_i^{\alpha}\cos(\vec{k}\cdot\vec{r}_i^{\alpha}))^2 +$$

$$(\sum_{i}^{N}\sum_{\alpha}^{m} S_i^{\alpha}\sin(\vec{k}\cdot\vec{r}_i^{\alpha}))^2] - \frac{\lambda}{\sqrt{\pi}}\frac{q^2}{\epsilon\sigma}\frac{\sigma}{L}\sum_{i}^{N}\sum_{\alpha}^{m}(S_i^{\alpha})^2 +$$

$$\frac{2\pi}{3}\frac{q^2\sigma}{\epsilon\sigma L}\left|\sum_{i}^{N}\sum_{\alpha}^{m} S_i^{\alpha}\frac{\vec{r}_i^{\alpha}}{L}\right|^2 + \sum_{i<j}^{N} 4\left[\left(\frac{\sigma}{r_{ij}}\right)^{12} - \left(\frac{\sigma}{r_{ij}}\right)^{6}\right] \quad (1)$$

where N is the total number of molecules, m is the number of sites per molecule (3 in this case with site number 3 being the oxygen site), ϵ and σ are the Lennard-Jones energy and size parameters, q is the hydrogen point charge value, r_{ij} is the magnitude of the space vector connecting molecules i and j, $r_{ij}^{\alpha\beta}$ is the magnitude of the space vector connecting site α in molecule i and site β in molecule j, L is the simulation box length, λ is a dimensionless number (set equal to 5.5 here) that controls the width of the Gaussian distribution and $\vec{k} = (2\pi/L)\vec{n}$ are the reciprocal vectors of the lattice for the Ewald method.[10] S^{α} is 1 for α = hydrogen and -2 for α = oxygen. In eq 1, the first term accounts for the interactions in the real space (original plus screening potential introduced by the Ewald method), the second term accounts for the fact that for the molecular system examined no interactions between different sites of the same molecule exist, the third term is a reciprocal space sum (canceling the screening potential), the fourth term is a self-term, and the fifth term is a surface term since a finite system is examined. In Table 1, the SPC and SPC/E parameter values are shown.

The functional form of eq 1 indicates that the system follows the corresponding states principle.[18] The quantity $q^2/(\epsilon\sigma)$, which multiplies all terms on the right-hand side of eq 1 except the Lennard-Jones term, defines an infinite number of different state points that correspond to the same reduced state point. As a result, one can use the original SPC/E (or SPC) parameter values in Table 1 to simulate a state point at a given temperature, T, and pressure, P (if the simulation is performed in the *NPT* ensemble), or at a given temperature, T, and density, ρ (if the simulation is performed in the *NVT* ensemble), and then, by keeping the $q^2/(\epsilon\sigma)$ and R_{OH}/σ ratios constant and modifying the individual q, ϵ, σ, and R_{OH} values, obtain a new state point without the need for additional simulations. The expressions that correlate thermodynamic properties between state points 1 and 2 and the corresponding molecular parameters are slightly more complicated than the corresponding expressions for the Lennard-Jones fluid.[10] They are given by the following equations

$$\frac{T_1}{T_2} = \frac{\epsilon_1}{\epsilon_2}$$

$$\frac{\rho_1}{\rho_2} = \left(\frac{\sigma_2}{\sigma_1}\right)^3 = \left(\frac{R_{OH,2}}{R_{OH,1}}\right)^3$$

$$\frac{P_1}{P_2} = \left(\frac{\sigma_2}{\sigma_1}\right)^3\frac{\epsilon_1}{\epsilon_2} = \left(\frac{\sigma_2 q_2}{\sigma_1 q_1}\right)^2 \quad (2)$$

where R_{OH} is the O−H bond length. The H−O−H bond angle remains unchanged in this transformation. This methodology provides an efficient way to reevaluate model parameters to obtain best agreement with experimental data for some given thermodynamic properties and is used in this work toward the optimization of the SPC/E and SPC parameters with respect to the pure water phase equilibrium.

TABLE 1: Parameter Values for the Molecular Models Examined in This Work

model parameter	SPC	SPC/E	MSPC/E
R_{OH} (Å)	1.0	1.0	0.9839
HOH angle (deg)	109.47	109.47	109.47
q (esu)	0.41	0.4238	0.4108
ϵ (kcal/mol)	0.155	0.155	0.148
σ (Å)	3.166	3.166	3.116

Simulation Details

In order that two phases be in equilibrium at a given temperature, the pressure in the two phases must be equal as well as the chemical potential of each component in the two phases. In this work, the phase equilibrium of pure water at different temperatures is calculated using the Gibbs ensemble Monte Carlo method.[11] Two different boxes are simulated simultaneously where the following moves are used: particle displacement, volume fluctuation, and particle interchange. These three moves are used according to the ratio: 84.5% particle displacement, 0.5% volume fluctuation and 15% particle interchange. The total number of water molecules in the two boxes, the total volume, and the temperature are kept constant throughout a simulation (GEMC−NVT calculation). In all cases, 200−250 water molecules are used in the simulation. A typical run consists of (4−6) × 10^6 moves for equilibration in the temperature range 300−400 K and (1−1.5) × 10^6 moves for equilibration at higher temperatures. In all cases, the equilibration stage is followed by (3−4) × 10^6 moves where thermodynamic properties are averaged. Initial configurations are based either on the fcc lattice with densities close to the

experimental values or on final configurations from previous runs carried out under similar conditions. For most of the state points examined, two simulation runs are performed.

Two two-body molecular potentials are used in the calculations, the SPC and the SPC/E models. To account for the electrostatic interactions exhibited by water partial charges, the full Ewald summation method is used with $\vec{n} = (n_x, n_y, n_z)$ and n_x, n_y, n_z assume integer values between 0 and 5. During the simulation, the average pressure of each phase is calculated explicitly using an equation derived from the molecular virial expression.[19] According to this equation,

$$P_{\text{Gibbs}} = \left\langle \frac{N}{V} k_B T \right\rangle_{\text{Gibbs}} - \left\langle \frac{\partial E_{\text{tot}}}{\partial V} \right\rangle_{\text{Gibbs}} \tag{3}$$

where

$$\begin{aligned}
3V\frac{\partial E_{\text{tot}}}{\partial V} = {} & q^2 \sum_{i<j}^{N} \sum_{\alpha}^{m} \sum_{\beta}^{m} S_i^{\alpha} S_j^{\beta} \left(2\frac{\lambda}{\sqrt{\pi}L} \exp\left(-\left(\frac{\lambda r_{ij}^{\alpha\beta}}{L} \right)^2 \right) \right) \left(1 - \frac{\vec{r}_{ij}^{\alpha\beta} \cdot \vec{r}_{ij}}{(r_{ij}^{\alpha\beta})^2} \right) - \\
& \operatorname{erfc}\left(\frac{\lambda r_{ij}^{\alpha\beta}}{L} \right) \frac{\vec{r}_{ij}^{\alpha\beta} \cdot \vec{r}_{ij}}{(r_{ij}^{\alpha\beta})^3} \Bigg) + \frac{q^2}{\sqrt{\pi}} \frac{\lambda}{L} \sum_{i}^{N} \sum_{\alpha}^{m} \sum_{\beta \neq \alpha}^{m} S_i^{\alpha} S_i^{\beta} \\
& \exp\left(-\left(\frac{\lambda r_{ii}^{\alpha\beta}}{L} \right)^2 \right) + \frac{q^2}{\sqrt{\pi}} \frac{\lambda}{L} \sum_{i}^{N} \sum_{\alpha}^{m} (S_i^{\alpha})^2 - \frac{2\pi q^2}{L^3} \sum_{\vec{k} \neq 0} \frac{1}{k^2} \\
& \exp\left(-\frac{k^2 L^2}{4\lambda^2} \right) \Bigg[\Bigg(\sum_{i}^{N} \sum_{\alpha}^{m} S_i^{\alpha} \cos(\vec{k} \cdot \vec{r}_i^{\alpha}) \Bigg)^2 + \\
& \Bigg(\sum_{i}^{N} \sum_{\alpha}^{m} S_i^{\alpha} \sin(\vec{k} \cdot \vec{r}_i^{\alpha}) \Bigg)^2 \Bigg] + \frac{4\pi q^2}{L^3} \sum_{\vec{k} \neq 0} \frac{1}{k^2} \\
& \exp\left(-\frac{k^2 L^2}{4\lambda^2} \right) \Bigg(\Bigg[\Bigg(\sum_{i}^{N} \sum_{\alpha}^{m} S_i^{\alpha} \cos(\vec{k} \cdot \vec{r}_i^{\alpha}) \Bigg) \Bigg(\sum_{j}^{N} \sum_{\alpha}^{m-1} S_j^{\alpha} (\vec{k} \cdot \vec{R}_{\text{OH},j}^{\alpha}) \\
& \sin(\vec{k} \cdot \vec{r}_j^{\alpha}) \Bigg) \Bigg] - \Bigg[\Bigg(\sum_{i}^{N} \sum_{\alpha}^{m} S_i^{\alpha} \sin(\vec{k} \cdot \vec{r}_i^{\alpha}) \Bigg) \Bigg(\sum_{j}^{N} \sum_{\alpha}^{m-1} S_j^{\alpha} (\vec{k} \cdot \vec{R}_{\text{OH},j}^{\alpha}) \\
& \cos(\vec{k} \cdot \vec{r}_j^{\alpha}) \Bigg) \Bigg] \Bigg) - \frac{2\pi q^2}{L^3} \left| \sum_{i}^{N} \sum_{\alpha}^{m} S_i^{\alpha} \vec{r}_i^{\alpha} \right|^2 + \\
& \frac{4\pi q^2}{3L^3} \Bigg(\sum_{i}^{N} \sum_{\alpha}^{m} S_i^{\alpha} \vec{r}_i^{\alpha} \Bigg) \cdot \Bigg(\sum_{i}^{N} \sum_{\alpha}^{m} S_i^{\alpha} \vec{r}_i \Bigg) + \\
& \sum_{i<j}^{N} 4\epsilon \left[12 \left(\frac{(\sigma)^{12}}{(r_{ij})^{13}} \right) - 6 \left(\frac{(\sigma)^6}{(r_{ij})^7} \right) \right] \frac{\vec{r}_{ij} \cdot \vec{r}_{ij}}{r_{ij}}
\end{aligned} \tag{4}$$

The average pressure is calculated during the simulation in both phases. However, in the liquid phase, large fluctuations occur so the vapor phase pressure is reported in all cases below.

Results and Discussion

Simulation data obtained in this work are reported in Tables 2−4. The simulation of water phase equilibria at relatively low temperature requires bias techniques to overcome problems related to low acceptance rates of insertion moves.[20,21] In this work, the excluded volume map sampling technique was used at low temperature in order to increase the successful insertion rate.[20] In Tables 2 and 3, experimental[22] and simulation data for the vapor pressure, saturated liquid and vapor densities, and liquid and vapor potential energy at saturation are reported using the SPC and SPC/E model. For the SPC model, calculations were limited to six different temperatures only, since this model has been studied in detail previously.[4] In Figures 2 and 3, the water coexistence curve and the vapor pressure curve are presented. Experimental data, simulation data from this work, and literature simulation data[4,23] are included for comparison. SPC predictions are in better agreement with experimental data than SPC/E predictions for the vapor pressure. This observation is in agreement with recent calculations by others.[24] On the other hand, SPC/E is more accurate for saturated liquid density, at least for the temperature range where calculations using both models are performed, and for saturated vapor density at elevated temperatures.

An attempt was made to improve agreement of molecular simulation with experimental data by reevaluating the molecular model parameters. Starting from the SPC/E parameters and maintaining the dimensionless ratio $q^2/\epsilon\sigma$ at the constant value of 121.4 and R_{OH}/σ at 0.3159, q, ϵ, σ, and R_{OH} parameter values were reevaluated and macroscopic properties were scaled according to eq 2. Different sets of parameters can accurately describe one of the macroscopic properties examined (vapor pressure, saturated liquid, and vapor density). However, none of these sets of parameters provide accurate predictions for all three properties simultaneously. Preliminary calculations with the SPC-based sets of molecular parameters showed similar behavior. In this case, $q^2/\epsilon\sigma = 113.7$ and $R_{OH}/\sigma = 0.3159$.

The accuracy of a molecular model for mixture predictions is very crucial for practical applications. A prerequisite for a model to be accurate for mixture vapor−liquid equilibria is that it provides accurate vapor pressure and reasonably good liquid density predictions for the pure components. In this respect, a set of SPC/E parameters (modified SPC/E−MSCP/E) is proposed that predicts vapor pressure and saturated liquid density values in fairly good agreement with experimental data. As shown in Table 4 and in Figures 2 and 3, the MSPC/E model predictions are superior to those from the SPC/E for vapor pressure for the temperature range examined. The average deviation between experimental and simulation data is 10% for the MSPC/E and 40% for the SPC/E model. On the other hand, average deviations for the saturated densities remain unchanged (5% for the liquid density and approximately 35% for the vapor density).

A thermodynamic property that strongly affects the vapor phase composition in mixture phase equilibria is the second virial coefficient of pure components. Estimation of the second virial coefficient is a relatively fast calculation based on the expression

$$B(T) = -\frac{1}{2} \langle \int [\exp(-E_{12}/kT) - 1] \mathrm{d}\vec{r}_{12} \rangle_{\Omega_1 \Omega_2} \tag{5}$$

where the average is taken over all the relative orientations of the two molecules denoted by $\Omega_1\Omega_2$.

In Figure 4, experimental data[25] and Monte Carlo results are presented for the pure water second virial coefficient over an extensive temperature range. Simulation results are only in qualitative agreement with the experimental data. SPC and MSPC/E predictions are significantly better than SPC/E, especially at low temperature.

The enthalpy of vaporization is calculated directly from the simulation results through the expression

TABLE 2: Vapor Pressure, Saturated Liquid and Vapor Densities, and Potential Energies Calculated by Gibbs Ensemble Monte Carlo Simulation Using the SPC Model and from Experimental Data[22]

	vapor pressure (bar)			saturated liquid density (g/cm^3)			saturated vapor density (g/cm^3)			saturated liquid potential energy (kcal/mol)	saturated vapor potential energy (kcal/mol)
T (K)	simulation	expt	% AD[a]	simulation	expt	% AD	simulation	expt	% AD	simulation	simulation
373.13	1.2 ± 0.2	1.0	22	0.904 ± 0.014	0.958	6	0.000770 ± 0.000139	0.000597	29	−8.90 ± 0.08	−0.14 ± 0.07
423.00	5.9 ± 0.6	4.7	24	0.850 ± 0.007	0.917	7	0.00353 ± 0.00033	0.00253	40	−8.26 ± 0.09	−0.48 ± 0.15
473.13	17.9 ± 1.2	15.6	15	0.765 ± 0.019	0.865	12	0.0114 ± 0.0008	0.00782	46	−7.47 ± 0.10	−0.90 ± 0.12
523.13	42.0 ± 3.0	39.8	6	0.663 ± 0.019	0.799	17	0.0277 ± 0.0085	0.0199	39	−6.70 ± 0.12	−1.33 ± 0.32
550.15	83.4 ± 10.1	61.4	36	0.563 ± 0.048	0.756	26	0.0639 ± 0.0143	0.0316	102	−6.00 ± 0.18	−2.13 ± 0.40
573.15	118.7 ± 11.0	85.9	38	0.446 ± 0.037	0.712	37	0.131 ± 0.013	0.0461	185	−5.28 ± 0.19	−3.14 ± 0.20

[a] % AD = percent absolute deviation.

TABLE 3: Vapor Pressure, Saturated Liquid and Vapor Densities, and Potential Energies Calculated by Gibbs Ensemble Monte Carlo Simulation Using the SPC/E Model and from Experimental Data[22]

	vapor pressure (bar)			saturated liquid density (g/cm^3)			saturated vapor density (g/cm^3)			saturated liquid potential energy (kcal/mol)	saturated vapor potential energy (kcal/mol)
T (K)	simulation	expt	% AD[a]	simulation	expt	% AD	simulation	expt	% AD	simulation	simulation
314.14	0.022 ± 0.003	0.08	72	0.987 ± 0.020	0.992	0.5	0.0000148 ± 0.0000014	0.000100	85	−10.87 ± 0.06	−0.01 ± 0.01
348.85	0.14 ± 0.01	0.40	64	0.949 ± 0.008	0.974	3	0.0000899 ± 0.0000073	0.000241	61	−10.40 ± 0.03	−0.06 ± 0.03
388.70	0.8 ± 0.1	1.7	53	0.932 ± 0.011	0.946	2	0.000466 ± 0.000080	0.000981	53	−9.81 ± 0.10	−0.15 ± 0.09
416.67	1.8 ± 0.1	4.0	55	0.903 ± 0.013	0.923	2	0.00100 ± 0.00011	0.00215	54	−9.50 ± 0.06	−0.22 ± 0.08
450.00	6.2 ± 0.4	9.3	34	0.874 ± 0.016	0.890	2	0.00339 ± 0.00020	0.00479	29	−9.04 ± 0.09	−0.42 ± 0.07
476.76	9.6 ± 0.9	16.8	43	0.834 ± 0.003	0.860	3	0.00506 ± 0.00055	0.00841	40	−8.70 ± 0.07	−0.54 ± 0.13
503.19	18.3 ± 3.3	28.0	35	0.790 ± 0.012	0.827	5	0.0104 ± 0.0011	0.0140	25	−8.30 ± 0.07	−1.26 ± 0.26
522.98	27.6 ± 6.1	39.7	30	0.773 ± 0.013	0.799	3	0.0156 ± 0.0008	0.0199	21	−8.08 ± 0.05	−1.21 ± 0.23
556.52	47.9 ± 5.4	67.5	29	0.703 ± 0.033	0.745	6	0.0346 ± 0.0010	0.0351	1	−7.49 ± 0.15	−1.92 ± 0.52
579.71	66.0 ± 8.9	94.2	30	0.612 ± 0.029	0.698	12	0.0473 ± 0.0064	0.0512	8	−6.81 ± 0.14	−1.64 ± 0.27
609.71	110.7 ± 12.0	140.0	21	0.527 ± 0.030	0.621	15	0.0952 ± 0.0178	0.0824	16	−6.20 ± 0.15	−2.79 ± 0.29

[a] % AD = percent absolute deviation.

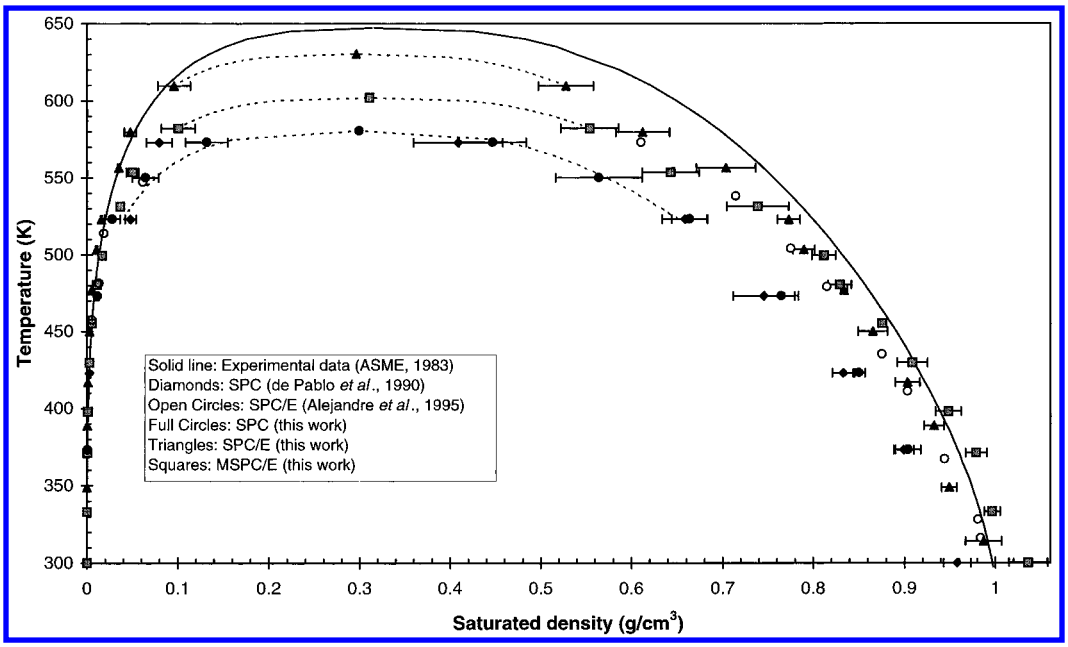

Figure 2. Pure water phase equilibria: experimental data[22] and simulation data calculated in this work and from the literature.

$$\Delta H_{l\rightarrow v} = U_{vap} - U_{liq} + P^{sat}\left(\frac{1}{\rho_{vap}} - \frac{1}{\rho_{liq}}\right) \qquad (6)$$

In Figure 5, experimental data[22] and simulation results are presented for the entire temperature range. At low and intermediate temperature, the MSPC/E model is in best agreement with experimental data compared to the other two models. As temperature increases above ≈530 K, significant deviations between SPC and MSPC/E models and experimental data are observed whereas SPC/E is in very good agreement with the experimental data. The deviation is due to the fact that both SPC and MSPC/E models predict a critical temperature value that is considerably lower than the experimental value (Table 5).

Simulation data at subcritical conditions are used to estimate the critical properties by invoking the following scaling law

$$\rho_l - \rho_v = A(T - T_c)^{\beta} \qquad (7)$$

and the law of rectilinear diameters

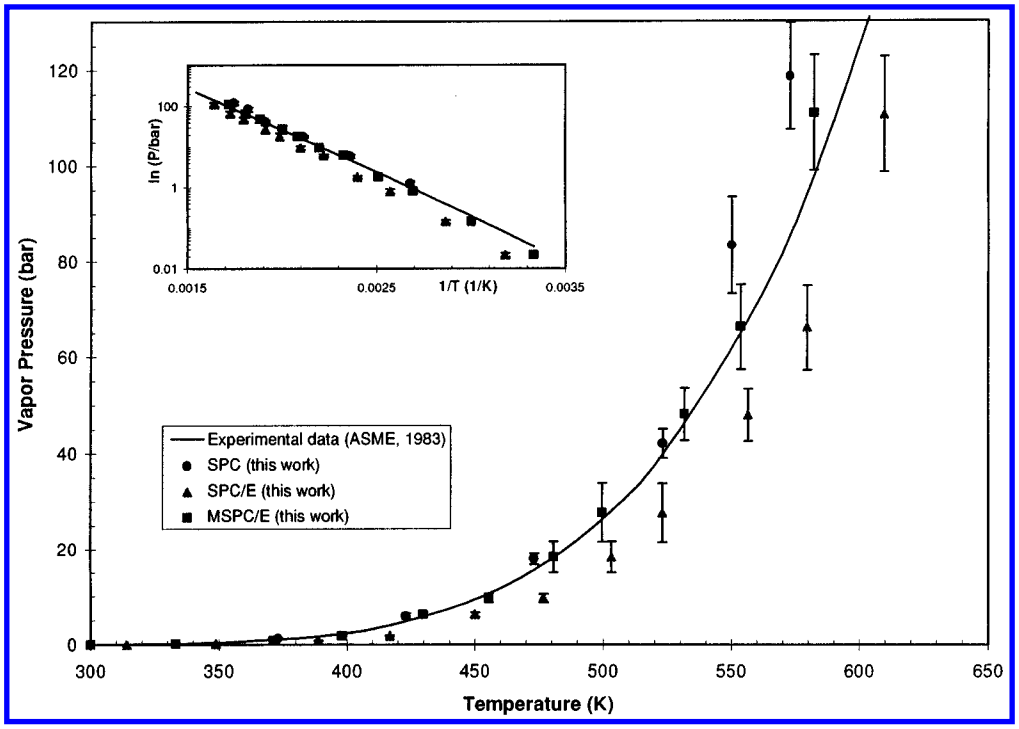

Figure 3. Pure water vapor pressure: experimental data[22] and simulation data calculated in this work.

TABLE 4: Vapor Pressure, Saturated Liquid and Vapor Densities, and Potential Energies Calculated by Gibbs Ensemble Monte Carlo Simulation Using the Modified-SPC/E (MSPC/E) Model and from Experimental Data[22]

	vapor pressure (bar)			saturated liquid density (g/cm^3)			saturated vapor density (g/cm^3)			saturated liquid potential energy (kcal/mol)	saturated vapor potential energy (kcal/mol)
T (K)	simulation	expt	% AD[a]	simulation	expt	% AD	simulation	expt	% AD	simulation	simulation
300.15	0.022 ± 0.003	0.035	38	1.036 ± 0.021	0.997	4	0.0000156 ± 0.0000015	0.000196	92	−10.38 ± 0.06	−0.01 ± 0.01
333.15	0.14 ± 0.01	0.20	29	0.996 ± 0.009	0.983	1	0.0000944 ± 0.0000076	0.000125	21	−9.93 ± 0.03	−0.06 ± 0.03
371.21	0.8 ± 0.1	0.9	14	0.979 ± 0.012	0.959	2	0.000489 ± 0.000084	0.000559	13	−9.37 ± 0.10	−0.14 ± 0.08
398.05	1.8 ± 0.1	2.3	22	0.948 ± 0.014	0.939	1	0.00105 ± 0.00012	0.00129	19	−9.07 ± 0.06	−0.21 ± 0.07
429.75	6.2 ± 0.4	5.7	10	0.918 ± 0.017	0.911	1	0.00356 ± 0.00020	0.00299	19	−8.63 ± 0.08	−0.40 ± 0.07
455.30	9.6 ± 0.9	10.5	9	0.875 ± 0.004	0.885	1	0.00531 ± 0.00058	0.00538	1	−8.31 ± 0.07	−0.51 ± 0.12
480.55	18.3 ± 3.3	18.1	1	0.829 ± 0.013	0.856	3	0.0109 ± 0.0011	0.00907	20	−7.92 ± 0.07	−1.21 ± 0.24
499.44	27.7 ± 6.2	26.1	6	0.811 ± 0.013	0.832	2	0.0164 ± 0.0008	0.0130	26	−7.72 ± 0.05	−1.15 ± 0.22
531.48	48.0 ± 5.4	45.7	5	0.738 ± 0.034	0.787	6	0.0363 ± 0.0010	0.0231	58	−7.16 ± 0.14	−1.84 ± 0.50
553.62	66.2 ± 8.9	64.7	2	0.642 ± 0.031	0.750	14	0.0496 ± 0.0067	0.0335	48	−6.50 ± 0.13	−1.57 ± 0.26
582.28	111.0 ± 12.0	97.6	14	0.553 ± 0.032	0.692	20	0.100 ± 0.019	0.0534	87	−5.92 ± 0.14	−2.67 ± 0.28

TABLE 5: Critical Properties for Water

model	critical temperature (K)	critical pressure (bar)	critical density (g/cm^3)	critical compressibility
experimental[22]	647.3	221.2	0.314	0.236
SPC				
this work	596	126	0.289	0.158
de Pablo et al.[4]	587		0.27	
Errington et al.[7]	593.8		0.2625	
SPC/E				
this work	630	148	0.295	0.172
Guissani and Guillot[5]	640	160	0.29	0.187
Alejandre et al.[23]	630		0.308	
Errington et al.[7]	639.0		0.2622	
MSPC/E	602	148	0.310	0.172

$$(\rho_l + \rho_v)/2 = \rho_c + B(T - T_c) \qquad (8)$$

with $\beta = 0.325$.[26] In Table 5, experimental data and simulation predictions for the critical properties are shown. Literature values for the same molecular models are included for comparison. The critical parameters estimated in this work from both SPC and SPC/E models are in reasonable agreement with the reported literature values, considering the relative deviation in the simulations. The SPC/E-predicted critical temperature is much closer than the SPC prediction to the experimental value, whereas both models predict similarly good critical density. Finally, the critical pressure from both models deviates considerably from the experimental value. Although the MSPC/E model is in good agreement with experimental data for the vapor pressure away from the critical point, the MSPC/E critical temperature, and consequently the critical pressure, is much lower than the experimental value. At the same time, the simulated critical density is in better agreement with experimental data than the SPC/E value. Both SPC and SPC/E models predict critical compressibility ($Z_c = P_c/(T_c\rho_c R)$) values that are way off the experimental value. The reevaluation of the SPC/E parameters has no effect on Z_c. This is an expected result since SPC/E and MSPC/E correspond to a molecular two-parameter corresponding states model (the variation of the three parameters, ϵ, σ, and q, is under the constraint $q^2/\epsilon\sigma$ = constant) that has a constant Z_c value. An analogy can be found in macroscopic models, as for example in the two-parameter van der Waals equation of state that has a constant $Z_c = 0.375$ for all fluids.

Finally, the structure of pure water is examined by calculating the oxygen−oxygen ($g_{O-O}(r)$), oxygen−hydrogen ($g_{O-H}(r)$), and

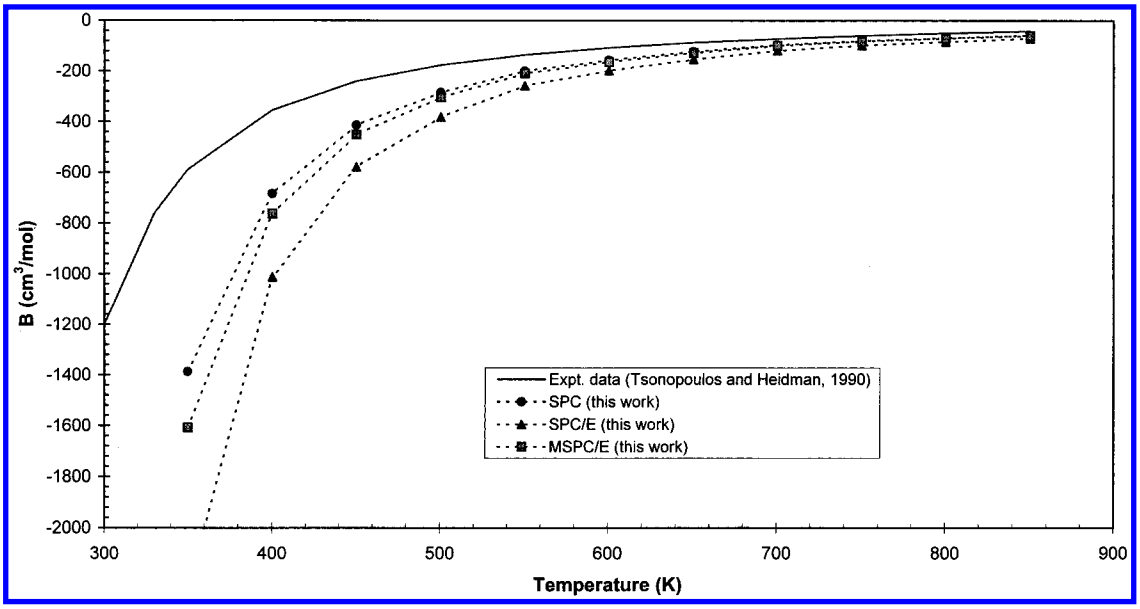

Figure 4. Pure water second virial coefficient: experimental data[25] and simulation data calculated in this work.

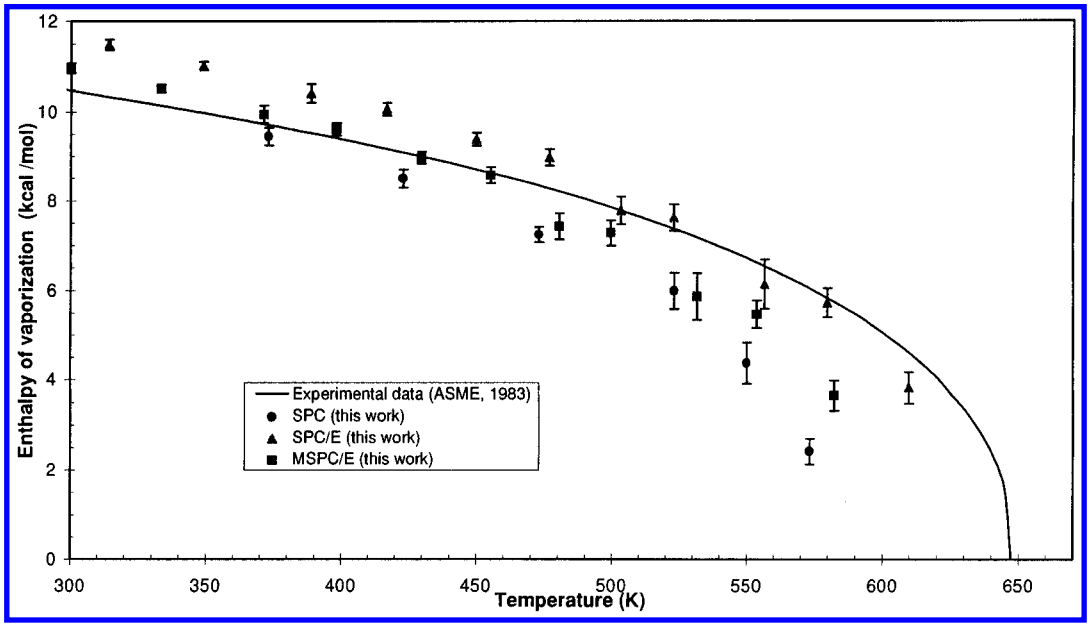

Figure 5. Pure water enthalpy of vaporization: experimental data[22] and simulation data calculated in this work.

hydrogen−hydrogen ($g_{H-H}(r)$) radial distribution functions (rdf). In Figure 6, Monte Carlo simulation results are shown at 298 K and 1 atm and 523 K and 60 atm for the three rdf from the SPC/E and MSPC/E models. The emphasis here is to show the effect of parameter change on the fluid structure, so SPC calculations are omitted and can be found elsewhere.[3] In Figure 6, experimental data are shown only for the 298 K[27] since there is a debate concerning the correctness of high-temperature experimental data.[28−30] In general, both models predict similar structures at both temperatures, in agreement with experimental data. A difference between the two models is the position of the first peak in the $g_{O-O}(r)$ rdf which is shifted to a lower position for the MSPC/E model (2.73 Å for the SPC/E, 2.71 Å for the MSPC/E, and 2.88 Å for the experimental data) due to the lower σ value for the new model (3.116 Å vs 3.166 Å for the SPC/E). The $g_{O-O}(r)$ rdf peak position calculated with the SPC/E model at 298 K is in excellent agreement with molecular dynamics calculations using the same model (2.72 Å).[31] In addition, calculations at 523 K are in good agreement with recently revised experimental data at 573 K and 95 atm (not shown in Figure 6).[30]

Conclusions

The phase equilibrium of pure water was calculated with Gibbs ensemble Monte Carlo simulation over a wide temperature range using simple molecular models that account explicitly for two-body interactions only. Vapor pressure and saturated liquid and vapor densities calculated in this work were compared with experimental data and literature simulation results. A new expression was derived for the calculation of pressure in systems where the Ewald method is used. To improve agreement of simulation with experimental data, a methodology was presented for the reevaluation of molecular model parameters. The new parameters result in improved prediction of the vapor pressure curve without any significant changes for the saturated densities. For the models examined, there is no unique set of parameters that can provide simultaneous good descriptions of the experimental vapor pressure and

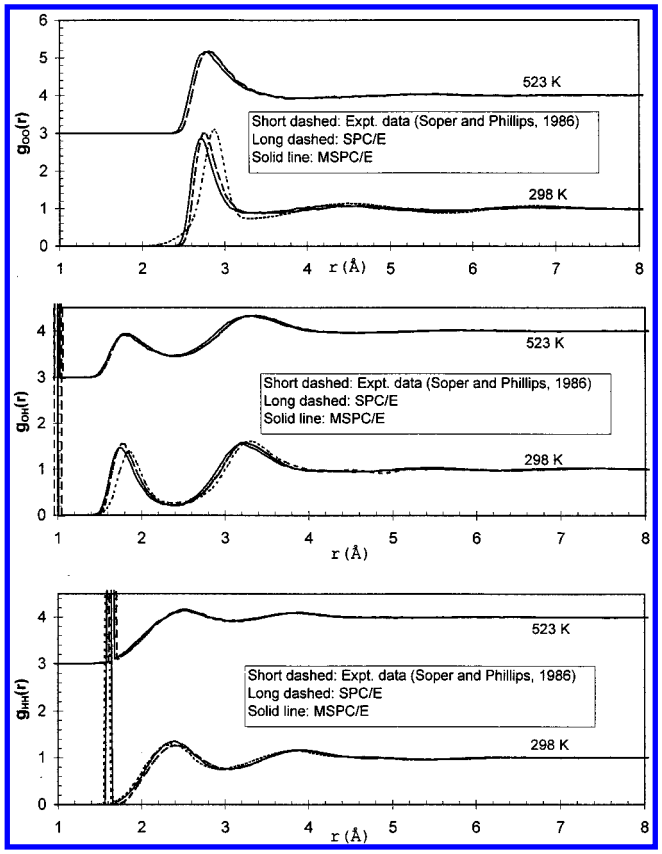

Figure 6. Pure water oxygen−oxygen ($g_{O-O}(r)$), oxygen−hydrogen ($g_{O-H}(r)$) and hydrogen−hydrogen ($g_{H-H}(r)$) radial distribution functions: experimental data[27] and simulation data calculated in this work.

saturated densities. Second virial coefficient, enthalpy of vaporization, and radial distribution functions were calculated from the different models and compared to experimental data. Critical properties were estimated from subcritical simulation data using critical scaling laws, and it was found that the SPC/E model results in good prediction for the critical temperature and critical density and that all models predict critical pressure values that are way off the experimental one.

Acknowledgment. We are grateful to Professor A. Z. Panagiotopoulos, Cornell University for very helpful discussions and for sharing his data prior to publication. Partial support of this project from NATO Collaborative Research Grants Program under grant number CRG 960966 is gratefully acknowledged.

References and Notes

(1) Shaw, R. W.; Brill, T. B.; Clifford, A. A.; Eckert C. A.; Franck E. U. *Chem. Eng. News* **1991**, Dec. *23*, 26.

(2) Panagiotopoulos, A. Z. In *Supercritical Fluids—Fundamentals for Application;* Kiran, E., Levelt Sengers, J. M. H., Eds.; Kluwer Academic Publishers: Dordrecht, 1994.

(3) Jorgensen, W. L.; Chandrasekhar, J.; Madura, J. D.; Impey, R. W.; Klein, M. L. *J. Chem. Phys.* **1983**, *79*, 926.

(4) de Pablo, J. J.; Prausnitz, J. M.; Strauch, H. J.; Cummings, P. T. *J. Chem. Phys.* **1990**, *93*, 7355.

(5) Guissani, Y.; Guillot, B. *J. Chem. Phys.* **1993**, *98*, 8221.

(6) Chialvo, A. A.; Cummings, P. T. *J. Chem. Phys.* **1996**, *105*, 8274.

(7) Errington, J. R.; Kiyohara, K.; Gubbins, K. E.; Panagiotopoulos, A. Z. *Fluid Phase Equil.*, in press.

(8) Berendsen, H. J. C.; Postma, J. P. M.; van Gunsteren, W. F.; Hermans, J. In *Intermolecular Forces;* Pullman, B., Ed.; Reidel: Dordrecht, 1981.

(9) Berendsen, H. J. C.; Grigera, J. R.; Straatsma, T. P. *J. Phys. Chem.* **1987**, *91*, 6269.

(10) Allen, M. P.; Tildesley, D. J. *Computer Simulation of Liquids*; Clarendon Press: Oxford, 1987.

(11) Panagiotopoulos, A. Z. *Mol. Phys.* **1987**, *61*, 813.

(12) Harris, J. G.; Yung, K. H. *J. Phys. Chem.* **1995**, *99*, 12021.

(13) Bernal, J. D.; Fowler, R. H. *J. Chem. Phys.* **1933**, *1*, 515.

(14) Ahlstrom, P.; Wallqvist, A.; Engström, S.; Jönsson, B. *Mol. Phys.* **1989**, *68*, 563.

(15) Caldwell, J.; Dang, L. X.; Kollman, P. A. *J. Am. Chem. Soc.* **1990**, *112*, 9144.

(16) Wallqvist, A.; Berne, B. J. *J. Chem. Phys.* **1993**, *97*, 13841.

(17) Chialvo, A. A. Personal communication, 1996.

(18) Prausnitz, J. M.; Lichtenthaler, R. N.; de Azevedo, E. G. *Molecular Thermodynamics of Fluid-Phase Equilibria*, 2nd ed.; Prentice Hall: Englewood Cliffs, NJ, 1986.

(19) Theodorou, D. N.; Boone, T. D.; Dodd, L. R.; Mansfield, K. F. *Makromol. Chem., Theory Simul.* **1993**, *2*, 191.

(20) Stapleton, M. R.; Panagiotopoulos, A. Z. *J. Chem. Phys.* **1990**, *92*, 1285.

(21) Shelley, J. C.; Patey, G. N. *J. Chem. Phys.* **1995**, *102*, 7656.

(22) ASME Steam Tables, 5th ed.; American Society of Mechanical Engineers: New York, 1983.

(23) Alejandre, J.; Tidlesley, D. J.; Chapela, G. A. *J. Chem. Phys.* **1995**, *102*, 4574.

(24) Harismiadis, V. I.; Panagiotopoulos, A. Z. Unpublished results, 1996.

(25) Tsonopoulos, C.; Heidman, J. L. *Fluid Phase Equil.* **1990**, *57*, 261.

(26) Levelt Sengers, J. M. H.; Straub, J.; Watanabe, K.; Hill, P. G. *J. Phys. Chem. Ref. Data* **1985**, *14*, 193.

(27) Soper, A. K.; Phillips, M. G. *Chem. Phys.* **1986**, *107*, 47.

(28) Postorino, P.; Tromp, R. H.; Ricci, M. A.; Soper, A. K.; Nellson, G. W. *Nature* **1993**, *366*, 668.

(29) Chialvo, A. A.; Cummings, P. T. *J. Phys. Chem.* **1996**, *100*, 1309.

(30) Soper, A. K.; Bruni, F.; Ricci, M. A. *J. Chem. Phys.* **1997**, *106*, 247.

(31) Svishchev, I. M.; Kusalik, P. G. *J. Chem. Phys.* **1993**, *99*, 3049.